Study of the $ZZ\gamma$ and $Z\gamma\gamma$ Couplings in $Z(\nu\nu)\gamma$ Production

S. Abachi,[14] B. Abbott,[28] M. Abolins,[25] B. S. Acharya,[43] I. Adam,[12] D. L. Adams,[37] M. Adams,[17] S. Ahn,[14] H. Aihara,[22] G. A. Alves,[10] E. Amidi,[29] N. Amos,[24] E. W. Anderson,[19] R. Astur,[42] M. M. Baarmand,[42] A. Baden,[23] V. Balamurali,[32] J. Balderston,[16] B. Baldin,[14] S. Banerjee,[43] J. Bantly,[5] J. F. Bartlett,[14] K. Bazizi,[39] A. Belyaev,[26] S. B. Beri,[34] I. Bertram,[31] V. A. Bezzubov,[35] P. C. Bhat,[14] V. Bhatnagar,[34] M. Bhattacharjee,[13] N. Biswas,[32] G. Blazey,[30] S. Blessing,[15] P. Bloom,[7] A. Boehnlein,[14] N. I. Bojko,[35] F. Borcherding,[14] J. Borders,[39] C. Boswell,[9] A. Brandt,[14] R. Brock,[25] A. Bross,[14] D. Buchholz,[31] V. S. Burtovoi,[35] J. M. Butler,[3] W. Carvalho,[10] D. Casey,[39] H. Castilla-Valdez,[11] D. Chakraborty,[42] S.-M. Chang,[29] S. V. Chekulaev,[35] L.-P. Chen,[22] W. Chen,[42] S. Choi,[41] S. Chopra,[24] B. C. Choudhary,[9] J. H. Christenson,[14] M. Chung,[17] D. Claes,[27] A. R. Clark,[22] W. G. Cobau,[23] J. Cochran,[9] W. E. Cooper,[14] C. Cretsinger,[39] D. Cullen-Vidal,[5] M. A. C. Cummings,[16] D. Cutts,[5] O. I. Dahl,[22] K. Davis,[2] K. De,[44] K. Del Signore,[24] M. Demarteau,[14] D. Denisov,[14] S. P. Denisov,[35] H. T. Diehl,[14] M. Diesburg,[14] G. Di Loreto,[25] P. Draper,[44] J. Drinkard,[8] Y. Ducros,[40] L. V. Dudko,[26] S. R. Dugad,[43] D. Edmunds,[25] J. Ellison,[9] V. D. Elvira,[42] R. Engelmann,[42] S. Eno,[23] G. Eppley,[37] P. Ermolov,[26] O. V. Eroshin,[35] V. N. Evdokimov,[35] T. Fahland,[8] M. Fatyga,[4] M. K. Fatyga,[39] J. Featherly,[4] S. Feher,[14] D. Fein,[2] T. Ferbel,[39] G. Finocchiaro,[42] H. E. Fisk,[14] Y. Fisyak,[7] E. Flattum,[25] G. E. Forden,[2] M. Fortner,[30] K. C. Frame,[25] S. Fuess,[14] E. Gallas,[44] A. N. Galyaev,[35] P. Gartung,[9] T. L. Geld,[25] R. J. Genik II,[25] K. Genser,[14] C. E. Gerber,[14] B. Gibbard,[4] S. Glenn,[7] B. Gobbi,[31] M. Goforth,[15] A. Goldschmidt,[22] B. Gómez,[1] G. Gómez,[23] P. I. Goncharov,[35] J. L. González Solís,[11] H. Gordon,[4] L. T. Goss,[45] A. Goussiou,[42] N. Graf,[4] P. D. Grannis,[42] D. R. Green,[14] J. Green,[30] H. Greenlee,[14] G. Grim,[7] S. Grinstein,[6] N. Grossman,[14] P. Grudberg,[22] S. Grünendahl,[39] G. Guglielmo,[33] J. A. Guida,[2] J. M. Guida,[5] A. Gupta,[43] S. N. Gurzhiev,[35] P. Gutierrez,[33] Y. E. Gutnikov,[35] N. J. Hadley,[23] H. Haggerty,[14] S. Hagopian,[15] V. Hagopian,[15] K. S. Hahn,[39] R. E. Hall,[8] S. Hansen,[14] J. M. Hauptman,[19] D. Hedin,[30] A. P. Heinson,[9] U. Heintz,[14] R. Hernández-Montoya,[11] T. Heuring,[15] R. Hirosky,[15] J. D. Hobbs,[14] B. Hoeneisen,[1,*] J. S. Hoftun,[5] F. Hsieh,[24] Ting Hu,[42] Tong Hu,[18] T. Huehn,[9] A. S. Ito,[14] E. James,[2] J. Jaques,[32] S. A. Jerger,[25] R. Jesik,[18] J. Z.-Y. Jiang,[42] T. Joffe-Minor,[31] K. Johns,[2] M. Johnson,[14] A. Jonckheere,[14] M. Jones,[16] H. Jöstlein,[14] S. Y. Jun,[31] C. K. Jung,[42] S. Kahn,[4] G. Kalbfleisch,[33] J. S. Kang,[20] R. Kehoe,[32] M. L. Kelly,[32] C. L. Kim,[20] S. K. Kim,[41] A. Klatchko,[15] B. Klima,[14] C. Klopfenstein,[7] V. I. Klyukhin,[35] V. I. Kochetkov,[35] J. M. Kohli,[34] D. Koltick,[36] A. V. Kostritskiy,[35] J. Kotcher,[4] A. V. Kotwal,[12] J. Kourlas,[28] A. V. Kozelov,[35] E. A. Kozlovski,[35] J. Krane,[27] M. R. Krishnaswamy,[43] S. Krzywdzinski,[14] S. Kunori,[23] S. Lami,[42] H. Lan,[14,†] R. Lander,[7] F. Landry,[25] G. Landsberg,[14] B. Lauer,[19] A. Leflat,[26] H. Li,[42] J. Li,[44] Q. Z. Li-Demarteau,[14] J. G. R. Lima,[38] D. Lincoln,[24] S. L. Linn,[15] J. Linnemann,[25] R. Lipton,[14] Q. Liu,[14,†] Y. C. Liu,[31] F. Lobkowicz,[39] S. C. Loken,[22] S. Lökös,[42] L. Lueking,[14] A. L. Lyon,[23] A. K. A. Maciel,[10] R. J. Madaras,[22] R. Madden,[15] L. Magaña-Mendoza,[11] S. Mani,[7] H. S. Mao,[14,†] R. Markeloff,[30] L. Markosky,[2] T. Marshall,[18] M. I. Martin,[14] K. M. Mauritz,[19] B. May,[31] A. A. Mayorov,[35] R. McCarthy,[42] J. McDonald,[15] T. McKibben,[17] J. McKinley,[25] T. McMahon,[33] H. L. Melanson,[14] M. Merkin,[26] K. W. Merritt,[14] H. Miettinen,[37] A. Mincer,[28] J. M. de Miranda,[10] C. S. Mishra,[14] N. Mokhov,[14] N. K. Mondal,[43] H. E. Montgomery,[14] P. Mooney,[1] H. da Motta,[10] C. Murphy,[17] F. Nang,[2] M. Narain,[14] V. S. Narasimham,[43] A. Narayanan,[2] H. A. Neal,[24] J. P. Negret,[1] P. Nemethy,[28] D. Nešić,[5] M. Nicola,[10] D. Norman,[45] L. Oesch,[24] V. Oguri,[38] E. Oltman,[22] N. Oshima,[14] D. Owen,[25] P. Padley,[37] M. Pang,[19] A. Para,[14] Y. M. Park,[21] R. Partridge,[5] N. Parua,[43] M. Paterno,[39] J. Perkins,[44] M. Peters,[16] R. Piegaia,[6] H. Piekarz,[15] Y. Pischalnikov,[36] V. M. Podstavkov,[35] B. G. Pope,[25] H. B. Prosper,[15] S. Protopopescu,[4] D. Pušeljić,[22] J. Qian,[24] P. Z. Quintas,[14] R. Raja,[14] S. Rajagopalan,[4] O. Ramirez,[17] P. A. Rapidis,[14] L. Rasmussen,[42] S. Reucroft,[29] M. Rijssenbeek,[42] T. Rockwell,[25] N. A. Roe,[22] P. Rubinov,[31] R. Ruchti,[32] J. Rutherfoord,[2] A. Sánchez-Hernández,[11] A. Santoro,[10] L. Sawyer,[44] R. D. Schamberger,[42] H. Schellman,[31] J. Sculli,[28] E. Shabalina,[26] C. Shaffer,[15] H. C. Shankar,[43] R. K. Shivpuri,[13] M. Shupe,[2] H. Singh,[9] J. B. Singh,[34] V. Sirotenko,[30] W. Smart,[14] A. Smith,[2] R. P. Smith,[14] R. Snihur,[31] G. R. Snow,[27] J. Snow,[33] S. Snyder,[4] J. Solomon,[17] P. M. Sood,[34] M. Sosebee,[44] N. Sotnikova,[26] M. Souza,[10] A. L. Spadafora,[22] R. W. Stephens,[44] M. L. Stevenson,[22] D. Stewart,[24] D. A. Stoianova,[35] D. Stoker,[8] M. Strauss,[33] K. Streets,[28] M. Strovink,[22] A. Sznajder,[10] P. Tamburello,[23] J. Tarazi,[8] M. Tartaglia,[14] T. L. T. Thomas,[31] J. Thompson,[23] T. G. Trippe,[22] P. M. Tuts,[12] N. Varelas,[25] E. W. Varnes,[22] D. Vititoe,[2] A. A. Volkov,[35] A. P. Vorobiev,[35] H. D. Wahl,[15] G. Wang,[15] J. Warchol,[32] G. Watts,[5] M. Wayne,[32] H. Weerts,[25] A. White,[44] J. T. White,[45] J. A. Wightman,[19] S. Willis,[30] S. J. Wimpenny,[9] J. V. D. Wirjawan,[45] J. Womersley,[14] E. Won,[39] D. R. Wood,[29] H. Xu,[5] R. Yamada,[14] P. Yamin,[4] C. Yanagisawa,[42] J. Yang,[28] T. Yasuda,[29] P. Yepes,[37]

 0031-9007/97/78(19)/3640(6)$10.00

C. Yoshikawa,[16] S. Youssef,[15] J. Yu,[14] Y. Yu,[41] Q. Zhu,[28] Z. H. Zhu,[39] D. Zieminska,[18] A. Zieminski,[18]
E. G. Zverev,[26] and A. Zylberstejn[40]
(DØ Collaboration)
[1]*Universidad de los Andes, Bogotá, Colombia*
[2]*University of Arizona, Tucson, Arizona 85721*
[3]*Boston University, Boston, Massachusetts 02215*
[4]*Brookhaven National Laboratory, Upton, New York 11973*
[5]*Brown University, Providence, Rhode Island 02912*
[6]*Universidad de Buenos Aires, Buenos Aires, Argentina*
[7]*University of California, Davis, California 95616*
[8]*University of California, Irvine, California 92697*
[9]*University of California, Riverside, California 92521*
[10]*LAFEX, Centro Brasileiro de Pesquisas Físicas, Rio de Janeiro, Brazil*
[11]*Centro de Investigación y de Estudios Avanzados, Mexico City, Mexico*
[12]*Columbia University, New York, New York 10027*
[13]*Delhi University, Delhi, India 110007*
[14]*Fermi National Accelerator Laboratory, Batavia, Illinois 60510*
[15]*Florida State University, Tallahassee, Florida 32306*
[16]*University of Hawaii, Honolulu, Hawaii 96822*
[17]*University of Illinois at Chicago, Chicago, Illinois 60607*
[18]*Indiana University, Bloomington, Indiana 47405*
[19]*Iowa State University, Ames, Iowa 50011*
[20]*Korea University, Seoul, Korea*
[21]*Kyungsung University, Pusan, Korea*
[22]*Lawrence Berkeley National Laboratory and University of California, Berkeley, California 94720*
[23]*University of Maryland, College Park, Maryland 20742*
[24]*University of Michigan, Ann Arbor, Michigan 48109*
[25]*Michigan State University, East Lansing, Michigan 48824*
[26]*Moscow State University, Moscow, Russia*
[27]*University of Nebraska, Lincoln, Nebraska 68588*
[28]*New York University, New York, New York 10003*
[29]*Northeastern University, Boston, Massachusetts 02115*
[30]*Northern Illinois University, DeKalb, Illinois 60115*
[31]*Northwestern University, Evanston, Illinois 60208*
[32]*University of Notre Dame, Notre Dame, Indiana 46556*
[33]*University of Oklahoma, Norman, Oklahoma 73019*
[34]*University of Panjab, Chandigarh 16-00-14, India*
[35]*Institute for High Energy Physics, 142-284 Protvino, Russia*
[36]*Purdue University, West Lafayette, Indiana 47907*
[37]*Rice University, Houston, Texas 77005*
[38]*Universidade Estadual do Rio de Janeiro, Rio de Janeiro, Brazil*
[39]*University of Rochester, Rochester, New York 14627*
[40]*Commissariat à L'Energie Atomique, Departement d'Astrophysique, Physique des Particules, Physique Nucleaire et d'Instrumentation Assocciee/Service de Physique des Particules, CE-SACLAY, Gif-sur-Yvette, France*
[41]*Seoul National University, Seoul, Korea*
[42]*State University of New York, Stony Brook, New York 11794*
[43]*Tata Institute of Fundamental Research, Colaba, Mumbai 400005, India*
[44]*University of Texas, Arlington, Texas 76019*
[45]*Texas A&M University, College Station, Texas 77843*
(Received 21 February 1997)

We have measured the $ZZ\gamma$ and $Z\gamma\gamma$ couplings by studying 13.1 pb^{-1} of $p\bar{p} \to \not{E}_t\gamma + X$ data at $\sqrt{s} = 1.8$ TeV with the DØ detector at the Fermilab Tevatron Collider. This is the first study of hadronic $Z\gamma$ production in the neutrino decay channel. Combining this measurement with our previous results using $Z \to ee$ and $\mu\mu$ yields the most stringent 95% C.L. limits to date on anomalous couplings: $|h_{30}^Z| < 0.4$, $|h_{40}^Z| < 0.06$ ($\Lambda = 750$ GeV). [S0031-9007(97)03134-7]

PACS numbers: 14.70.Hp, 13.40.Em, 13.40.Gp, 13.85.Qk

In the standard model (SM), couplings of the form $ZV\gamma$, where V is a Z or γ, vanish at tree level. A direct measurement of the $ZV\gamma$ couplings is possible by studying $Z\gamma$ production. Previously, only the charged lepton decay modes of the Z have been studied in $p\bar{p}$ collisions at the Fermilab Tevatron ($\sqrt{s} = 1.8$ TeV) [1,2]. Here we report the first measurement of $Z\gamma$ production in the invisible (neutrino) decay channel of the Z at a

hadron collider; such studies have recently been made at LEP [3,4]. This analysis of the neutrino decay channel significantly improves the limits on $ZZ\gamma$ and $Z\gamma\gamma$ trilinear couplings and, in combination with previous DØ limits from other decay channels [2], gives stringent new limits.

We have studied the reaction $p\bar{p} \to \not{E}_T\gamma + X$ (where $\not{E}_T$ is missing transverse energy) using data from the 1992–1993 Tevatron run with the DØ detector, corresponding to an exposure of 13.1 ± 0.7 pb^{-1}. The advantages of using the $Z \to \nu\nu$ mode compared with the $\ell^+\ell^-$ decay channels are larger geometrical acceptance and detection efficiency; higher branching ratio (by a factor of 6 over ee or $\mu\mu$); and absence of the radiative Z-decay contribution. However, the invisible decay mode of the Z does not allow reconstruction of the Z mass and has larger potential background.

The DØ detector, described in detail elsewhere [5], consists of three main systems. Central and forward drift chambers are used to identify charged tracks for $|\eta| \leq 3.2$, where η is pseudorapidity. The calorimeter consists of uranium-liquid argon sampling detectors with fine segmentation in a central and two end cryostats, and provides near-hermetic coverage for $|\eta| \leq 4.4$. The energy resolution of the calorimeter was measured in beam tests [6] to be $15\%/\sqrt{E}$ for electrons and $50\%/\sqrt{E}$ for isolated pions (E in GeV). The calorimeter towers subtend 0.1×0.1 in $\eta \times \phi$ (ϕ is the azimuthal angle), segmented longitudinally into four electromagnetic (EM) and four or five hadronic layers. In the third EM layer, at the EM shower maximum, the cells are 0.05×0.05 in $\eta \times \phi$. The muon system consists of magnetized iron toroids with one inner and two outer layers of drift tubes, providing coverage for $|\eta| \leq 3.3$. For this analysis the muon detector was used only as a veto.

$Z\gamma$ candidates were selected by requiring a significant amount of $\not{E}_T$ and an isolated photon with high transverse energy (E_T^γ). There are three major sources of background to $\not{E}_T\gamma$ production: (1) jet (j) related background from jj and $j\gamma$ production, occurring when a jet hits a poorly instrumented region of the detector resulting in mismeasured $\not{E}_T$. In the dijet case, one jet additionally has to be reconstructed as a photon when fragmenting into a leading neutral meson; (2) cosmic ray or beam halo muon bremsstrahlung in the EM calorimeter which results in a reconstructed single photon in the event with balancing missing energy; (3) W boson production (with $W \to e\nu$), where the electron is reconstructed as a photon due to inefficiency of the tracking chambers. Other backgrounds, such as $W(\mu\nu) + j$ or $Z(\nu\nu) + j$ production with a jet faking a photon (and an unreconstructed or forward muon for the W case) are negligible.

The $\not{E}_T\gamma$ sample was obtained with a trigger which required an isolated EM cluster with $E_T \geq 20$ GeV. A photon cluster was required to be within the fiducial region of the calorimeter and tracking chambers [$|\eta| \leq 1.0$ in the central calorimeter (CC) or $1.5 \leq |\eta| \leq 2.5$ in the end calorimeters (EC)]. The off-line photon identification requirements were: (i) EM energy >0.96 times the total shower energy; (ii) lateral and longitudinal shower shape consistent with that of an electron shower [5]; (iii) the isolation variable of the cluster [2] <0.1; (iv) a photon cluster with no associated tracks or hits in the drift chambers; (v) development of the photon shower in the EM calorimeter consistent with its origin at the interaction vertex reconstructed by the tracking chambers; (vi) no muon tracks in the central calorimeter near the photon; (vii) no additional EM clusters in the event with $E_T > 5$ GeV; and (viii) $E_T^\gamma > 40$ GeV.

Missing transverse energy was calculated using the calorimeter energy deposits [5] and was shown to reproduce well the W boson event properties [7]. The hadronic calorimeter energy response was determined by minimizing the average $\not{E}_T$ in inclusive $Z \to ee$ events. The resolution of the $\not{E}_T$ projected on a given axis was $\approx$6 GeV and depended slightly on the transverse boost of the $Z\gamma$ system. We required $\not{E}_T$ to exceed 40 GeV. We also required no reconstructed muons in the central region of the detector ($|\eta_\mu| < 1.0$) and no hadronic jets in the event with transverse energies above 15 GeV.

This selection resulted in four $Z(\nu\nu)\gamma$ candidates. Three events had a photon in the CC and one in the EC. The highest photon E_T in this sample was 68 GeV.

To estimate the number of surviving jet-related background events, we first determined the probability to mismeasure $\not{E}_T$ in the detector by comparing the numbers of $\not{E}_T j$ and jj events collected with a single jet trigger. This probability falls exponentially with $\not{E}_T$ and is $<10^{-4}$ for $\not{E}_T > 35$ GeV. The probability for a jet to fake a photon was measured [2,8] to be $(7 \pm 2) \times 10^{-4}$. These probabilities were applied to the $j\gamma + X$ cross section [9] and $jj + X$ cross section (calculated from data) with a minimum transverse energy cut of 40 GeV imposed on jets and photons. The total background from these sources was estimated to be <0.6 events.

The muon bremsstrahlung background was significantly suppressed by the photon quality criteria (v) and (vi), as well as by the high E_T^γ cut and the central muon veto. (The muon veto was not applied in the forward region due to high chamber occupancy.) Muon bremsstrahlung backgrounds were reduced by requiring that the photon direction deduced from the finely divided EM calorimeter be consistent with the event vertex location (v). The photon impact parameter resolution was 10–20 cm. Additional suppression of the cosmic ray background was achieved by rejecting events with a muonlike energy deposition in the vicinity of the photon cluster (vi). The residual background was estimated by applying the photon quality cuts to very clean samples of muon bremsstrahlung events. The estimated total muon background is 1.8 ± 0.6 events.

The $W \to e\nu$ background was suppressed by the E_T^γ and $\not{E}_T$ cuts, set above the Jacobian peak for $W \to e\nu$ decays, and by the jet veto which decreased the smearing of the Jacobian peak due to associated jet production. It was further reduced by the photon quality cut (iv)

which rejected photons with associated tracks or hits in the tracking chambers within roads pointing to the EM cluster. The rejection power of these cuts was estimated using $Z \to ee$ and $W \to e\nu$ samples with electrons reconstructed as photons due to the absence of a track. The residual background was estimated using the $W \to e\nu$ sample with the cuts similar to the ones used for signal (except that a reconstructed track was required to match the EM cluster). The number of background events, obtained by applying track- and hit-counting rejection factors to this sample, was estimated to be 4.0 ± 0.8 events.

The total muon and $W \to e\nu$ background is 5.8 ± 1.0 events. Since the total jet-related background was less than the error on the dominant backgrounds, it was (conservatively) neglected when deriving the limits on the couplings. Table I summarizes the backgrounds.

The acceptance of the DØ detector for the $\nu\nu\gamma$ final state was determined using the leading order event generator [10] to generate 4-vectors for the $Z\gamma$ processes as a function of the coupling parameters. The 4-vectors were used as input to a fast detector simulation program which modeled the effects of the EM and missing transverse energy resolutions, interaction vertex spread, and off-line efficiencies. The efficiencies were estimated primarily by using $Z \to ee$ data. The trigger was fully efficient for $E_T^\gamma > 40$ GeV. The overall efficiency of the photon selection cuts was 0.57 ± 0.03 (0.64 ± 0.05) in CC (EC). The geometrical acceptance was 80% for the SM case and increased slightly for nonzero couplings. The MRSD-′ [11] set of parton distribution functions (pdf) was used in the calculations. The uncertainty due to the choice of pdf (6%, determined by using different pdf choices) was included in the systematic error of the Monte Carlo (MC) calculation. We accounted for the effect of higher order QCD corrections by multiplying the rates by a constant factor $k = 1.34$ [10]. The jet veto efficiency was estimated to be 0.84 ± 0.02 by applying the requirement of no hadronic jets with $E_T > 15$ GeV to the inclusive $Z \to ee$ data. The value of the k factor and the efficiency of the jet veto were shown to be consistent with the NLL $Z\gamma$ MC [12] for the SM couplings.

The expected signal for SM couplings is $1.8 \pm 0.2 \pm 0.1$ events, where the first error is due to the uncertainty in the MC modeling (13%), and the second is the uncertainty in the integrated luminosity calculation (5.4%). Our observed signal agrees within the errors with the background expectation plus the SM prediction. We verified this by simultaneously modifying the cuts on E_T^γ and $\not\!\!E_T$ to 35 or 45 GeV; in both cases the observed number of events agreed well with the predictions. The E_T^γ and $\not\!\!E_T$ spectra of the candidates along with the SM prediction and estimated background are shown in Fig. 1.

TABLE I. Summary of signal and backgrounds.

	CC	EC	Total
Candidates	3	1	4
Muon background	1.4 ± 0.6	0.4 ± 0.2	1.8 ± 0.6
$W \to e\nu$ background	2.2 ± 0.6	1.8 ± 0.6	4.0 ± 0.8
$jj + j\gamma$ background	< 0.4	< 0.2	< 0.6
Total background	3.6 ± 0.8	2.2 ± 0.6	5.8 ± 1.0
SM signal prediction	1.4 ± 0.2	0.4 ± 0.1	1.8 ± 0.2

The most general Lorentz and gauge invariant $ZV\gamma$ vertex is described by four coupling parameters h_i^V [13]. Combinations of the CP-conserving (CP-violating) parameters h_3^V and h_4^V (h_1^V and h_2^V) correspond to the electric (magnetic) dipole and magnetic (electric) quadrupole transition moments of the $ZV\gamma$ vertex. Nonzero (anomalous) values of the h_i^V couplings result in an increase of the $Z\gamma$ production cross section, particularly for large E_T^γ [10]. Partial wave unitarity of the general $f\bar{f} \to Z\gamma$ process restricts the $ZV\gamma$ couplings uniquely to their vanishing SM values at asymptotically high energies [14]. Therefore, the coupling parameters must be modified by form factors $h_i^V = h_{i0}^V/(1 + \hat{s}/\Lambda^2)^n$, where $\hat{s}$ is the square of the invariant mass of the $Z\gamma$ system, Λ is the form-factor scale, and h_{i0}^V are coupling values at the low energy limit [10]. We take $n = 3$ for $h_{1,3}^V$ and $n = 4$ for $h_{2,4}^V$ [10]. This choice yields the same asymptotic energy behavior for all of the couplings. Unlike $W\gamma$ production where form-factor effects do not play a crucial role, the Λ-dependent effects cannot be ignored in $Z\gamma$ production at Tevatron energies. This is due to the higher power of $\hat{s}$ in the vertex function, a direct consequence of the additional Bose-Einstein symmetry of the $ZV\gamma$ vertices [10].

To set limits on the anomalous couplings, a fit to the observed E_T spectrum of the photon with the MC signal prediction plus estimated background was done. The fit was performed using a binned likelihood method [8], with Poisson statistics for the signal and Gaussian uncertainties for background, luminosity, and efficiencies. Because the contribution of the anomalous couplings is concentrated in

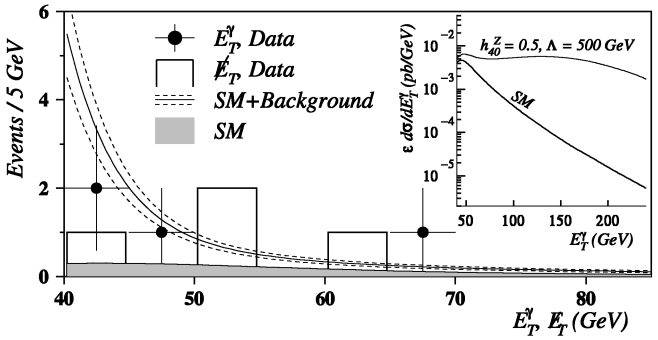

FIG. 1. Transverse energy spectrum of photons in the $\not\!\!E_T\gamma$ events. The points show the data; the hatched curve is the SM signal prediction; the solid line is the sum of the SM signal prediction and the background, with the errors shown by the band. The histogram shows the $\not\!\!E_T$ distribution of the candidate events (not used in the fit). The inset shows the predicted $d\sigma/dE_T^\gamma$ folded with the efficiencies for SM and anomalous couplings.

the high E_T^γ region, the differential distribution $d\sigma/dE_T^\gamma$ is more sensitive to the anomalous couplings than the total cross section (see inset in Fig. 1 and Ref. [10]). To exploit the fact that anomalous coupling contributions lead to an excess of events with a high E_T photon, a high-E_T^γ bin, with no events observed, was explicitly included in the fit [8].

The one- and two-degree of freedom (DOF) 95% C.L. limits on anomalous couplings in the (h_{30}^Z, h_{40}^Z) plane were obtained by cutting the likelihood function 1.92 or 3.00 units below the maximum. A form-factor scale of $\Lambda = 500$ GeV was used in these calculations. The two-DOF limit contour [see Fig. 2(a)] represents the *correlated* limit on a pair of couplings when both are allowed to vary independently. For models which predict a particular relationship between the couplings, thus eliminating one DOF, the appropriate point on the one-DOF limit contour should be used. The limit on one coupling when all others are fixed at the SM values is given by the intersection of this contour with the corresponding axis (*axis* limit). Since the (h_{30}^Z, h_{40}^Z) pair is nearly uncorrelated with the other pairs [2] the correlated limits in the above plane are a good approximation of the *global* limits, i.e., limits independent of the values of other couplings. In what follows only axis limits are quoted; the correlated limits can be obtained from the figures. The 95% C.L. axis limits for the *CP*-conserving $ZZ\gamma$ and $Z\gamma\gamma$ couplings from this measurement are listed in Table II. Limits on a *CP*-violating pair of couplings are numerically the same as for the corresponding *CP*-conserving pair.

Combined limits on anomalous couplings were also obtained based on this measurement and previous DØ results [2] using $Z \to ee, \mu\mu$. Errors common to both analyses (e.g., luminosity, pdf uncertainties) were taken into account when combining the results. The combined 95% C.L. limits are about 10% tighter than for the neutrino channel alone and are listed in Table II.

Finally, the sensitivity of this measurement to the value of the form-factor scale Λ was studied. The value $\Lambda = 500$ GeV chosen above is close to the sensitivity limit of the previous Tevatron measurements [1,2]. The sensitivity of the present measurement is higher and reaches $\Lambda = 750$ GeV for the neutrino channel alone (slightly higher for the combined $ee + \mu\mu + \nu\nu$ channels). The 95% C.L. limits obtained for $\Lambda = 750$ GeV are much tighter (see Table II) and are shown in Fig. 2(b).

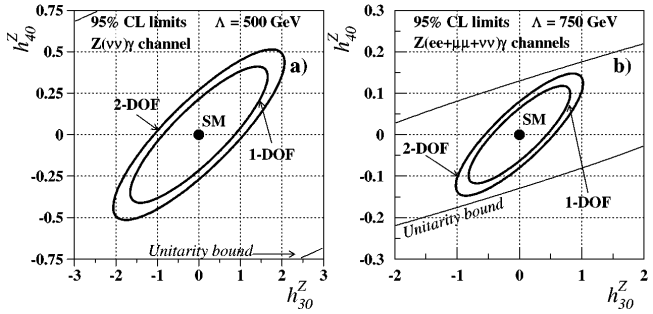

FIG. 2. Limits on the correlated *CP*-conserving anomalous $ZZ\gamma$ coupling parameters h_{30}^Z and h_{40}^Z for (a) $Z(\nu\nu)\gamma$ ($\Lambda = 500$ GeV) and (b) $Z(ee + \mu\mu + \nu\nu)\gamma$ ($\Lambda = 750$ GeV). The solid ellipses represent 95% C.L. one- and two-DOF exclusion contours. The thin lines show unitarity bounds.

It is important to extend the experimental sensitivity to high values of the form-factor scale which is closely related to the scale of the new physics which can produce anomalous couplings. Our results show that the sensitivity of direct measurements of $Z\gamma$ production to anomalous couplings grows with Λ. This fact makes such measurements complementary to the direct searches for new physics which have higher sensitivity at low scales. The limits on h_{40}^V and h_{20}^V couplings for $\Lambda = 750$ GeV obtained in this measurement are already close to expectations for anomalous couplings from new physics (see, e.g., [15]) and are the most stringent limits on anomalous $ZV\gamma$ couplings currently available.

We thank U. Baur and J. Ohnemus for MC programs and helpful discussions. We thank the staffs at Fermilab and collaborating institutions for their contributions to this work, and acknowledge support from the Department of Energy and National Science Foundation (U.S.A.), Commissariat à L'Energie Atomique (France), State Committee for Science and Technology and Ministry for Atomic Energy (Russia), CNPq (Brazil), Departments of Atomic Energy and Science and Education (India), Colciencias (Colombia), CONACyT (Mexico), Ministry of Education and KOSEF (Korea), CONICET and UBACyT (Argentina), and the A.P. Sloan Foundation.

TABLE II. 95% C.L. axis limits on the *CP*-conserving anomalous couplings h_{30}^V, h_{40}^V. Limits on the *CP*-violating partners h_{10}^V, h_{20}^V are numerically the same.

Channel	$h_{40}^Z = 0$	$h_{30}^Z = 0$	$h_{40}^\gamma = 0$	$h_{30}^\gamma = 0$
		$\Lambda = 500$ GeV		
$\nu\nu$	$\lvert h_{30}^Z\rvert < 0.87$	$\lvert h_{40}^Z\rvert < 0.21$	$\lvert h_{30}^\gamma\rvert < 0.90$	$\lvert h_{40}^\gamma\rvert < 0.22$
$ee, \mu\mu, \nu\nu$	$\lvert h_{30}^Z\rvert < 0.78$	$\lvert h_{40}^Z\rvert < 0.19$	$\lvert h_{30}^\gamma\rvert < 0.81$	$\lvert h_{40}^\gamma\rvert < 0.20$
		$\Lambda = 750$ GeV		
$\nu\nu$	$\lvert h_{30}^Z\rvert < 0.49$	$\lvert h_{40}^Z\rvert < 0.07$	$\lvert h_{30}^\gamma\rvert < 0.50$	$\lvert h_{40}^\gamma\rvert < 0.07$
$ee, \mu\mu, \nu\nu$	$\lvert h_{30}^Z\rvert < 0.44$	$\lvert h_{40}^Z\rvert < 0.06$	$\lvert h_{30}^\gamma\rvert < 0.45$	$\lvert h_{40}^\gamma\rvert < 0.06$

*Visitor from IHEP, Beijing, China.
†Visitor from Univ. San Francisco de Quito, Ecuador.

[1] CDF Collaboration, F. Abe *et al.,* Phys. Rev. Lett. **74**, 1941 (1995).
[2] DØ Collaboration, S. Abachi *et al.,* Phys. Rev. Lett. **75**, 1028 (1995).
[3] L3 Collaboration, M. Acciarri *et al.,* Phys. Lett. B **346**, 190 (1995).
[4] DELPHI Collaboration, P. Abreu *et al.,* Phys. Lett. B **380**, 471 (1996).
[5] DØ Collaboration, S. Abachi *et al.,* Nucl. Instrum. Methods Phys. Res., Sect. A **338**, 185 (1994).
[6] DØ Collaboration, S. Abachi *et al.,* Nucl. Instrum. Methods Phys. Res., Sect. A **324**, 53 (1993).
[7] M. Rijssenbeek (for the DØ and CDF Collaborations), Report No. Fermilab–Conf–96/365–E, in Proceedings of the 28th International Conference on HEP, Warsaw, Poland, 1996 (to be published).
[8] G. Landsberg, Ph.D. dissertation, SUNY at Stony Brook, 1994 (unpublished).
[9] H. Baer, J. Ohnemus, and J. F. Owens, Phys. Rev. D **42**, 61 (1990).
[10] U. Baur and E. L. Berger, Phys. Rev. D **47**, 4889 (1993).
[11] A. D. Martin, R. G. Roberts, and W. J. Stirling, Phys. Lett. B **306**, 145 (1993); **309**, 492(E) (1993).
[12] J. Ohnemus, Phys. Rev. D **47**, 940 (1993); **51**, 1068 (1995).
[13] K. Hagiwara *et al.,* Nucl. Phys. **B282**, 253 (1987).
[14] K. Hagiwara and D. Zeppenfeld, Nucl. Phys. **B274**, 1 (1986); U. Baur and D. Zeppenfeld, Phys. Lett. B **201**, 383 (1988).
[15] D. Chang, W.-Y. Keung, and P. Pal, Phys. Rev. D **51**, 1326 (1995).